

Study on Energy Absorption Characteristic of Cab Frame with FEM

Shigeyuki Haruyama, Oke Oktavianty, Zefry Darmawan, Tadayuki Kyoutani, Ken Kaminishi

Abstract—Cab's frame strength is considered as an important factor in excavator's operator safety, especially during roll-over. In this study, we use a model of cab frame with different thicknesses and perform elastoplastic numerical analysis by using Finite Element Method (FEM). Deformation mode and energy absorption's of cab's frame part are investigated on two conditions, with wrinkle and without wrinkle. The occurrence of wrinkle when deforming cab frame can reduce energy absorption, and among 4 parts with wrinkle, the energy absorption significantly decreases in part C. Residual stress that generated upon the bending process of part C is analyzed to confirm it possibility in increasing the energy absorption.

Keywords—ROPS, FEM, hydraulic excavator, cab frame, energy absorption.

I. INTRODUCTION

RECENTLY, construction machines have been commonly provided with a cab structure that is configured to protect an operator when the machines fall down. Hydraulic excavator scaffolds may use in unstable land or slopes, with a tipped over or roll over risk. Roll-Over Protective Structure (ROPS) standards have been established and considered as an important factor to protect occupant when hydraulic excavator falls. Operator's seat must be secured to passenger space in cab frame. It is necessary to withstand impact because of fall with increasing frame strength [1]-[5].

Cab frame of hydraulic excavator which was intended to isolate the occupants from wind and rain, will crushed upon fall, and this may be dangerous to passenger. The danger comes from the impact energy that transmitted to the excavator occupant. To increase passenger safety, the impact energy transmitted should be as low as possible. To minimize the impact energy, it is necessary to dissipate the energy that comes because of tipped over or rolled over by absorbing the energy through deformation of excavator structure.

To increase cab frame strength, the structural change by adding the thickness and material change has been done. Nevertheless, then, the production cost of cab frame will increase. The necessity to perform analysis during development to reduce development period and cost are discussed [6]. In this study, we use a model of cab frame with varying thickness and

Shigeyuki Haruyama and Ken Kaminishi are with graduate School of Innovation & Technology Management, Yamaguchi University, Ube, Japan (e-mail: haruyama@yamaguchi-u.ac.jp, kaminisi@yamaguchi-u.ac.jp).

Oke Oktavianty and Zefry Darmawan are with Department of Mechanical Engineering, Yamaguchi University, Japan and lecturer at Industrial Engineering Department, University of Brawijaya, Indonesia (e-mail: u504wc@yamaguchi-u.ac.jp, v501wc@yamaguchi-u.ac.jp).

Tadayuki Kyoutani is with Graduate School of Science and Technology, Department of Mechanical Engineering, Yamaguchi University, Ube, Japan.

we performed elastoplastic numerical analysis with FEM. While generating local wrinkle, a thin cylindrical tube that is mainly used as automotive body structure, can absorb energy [7]. Residual stresses are the stresses that remained in a solid material after the original cause of the stresses has been removed. Residual stresses can occur through a variety of mechanisms such as bending, welding etc. Residual stresses due to bending process is discussed and analyzed [8], [9]. In this study, wrinkle occurrence effect to energy absorption in deformation mode on each part is investigated. Effect of energy absorption characteristics by residual stress that generated upon bending process is discussed.

II. ENERGY ABSORPTION CHARACTERISTIC

A. Condition Analysis

An elastoplastic numerical analysis of cab frame with general-purpose analysis software is performed by using MSC. Marc software. The analysis model is shown in Fig. 1.

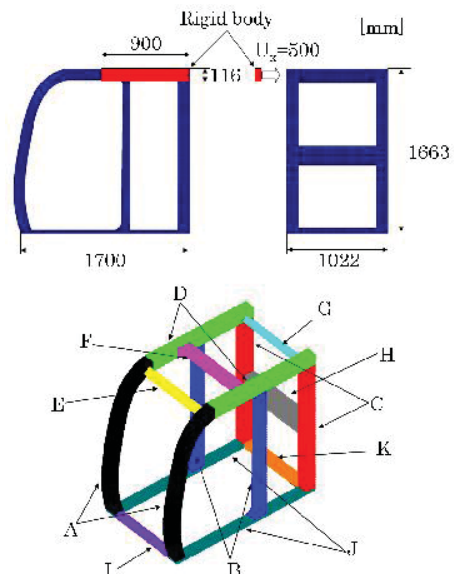


Fig. 1 Analysis model

Analysis model is created by combining a cylindrical part of quadrilateral axisymmetric shell elements. The frame is classified into 11 parts namely A ~ K. The boundary condition of frame bottom surface in 4 corners is completely restrained as shown in Fig. 2. A rigid wall (116 mm × 900 mm) beside part D with forced displacement 500 mm is allowed to collapse the model. The material properties of cab frame are homogeneous and isotropic of elastic-plastic. Stress-strain relationship is

assumed according to two straight hardening rules as shown in (1):

$$\begin{aligned} \sigma &= E\varepsilon \quad [\varepsilon < \sigma_y/E] \\ \sigma &= \sigma_y + E_h(\varepsilon - \sigma_y/E), \quad [\varepsilon > \sigma_y/E] \end{aligned} \quad (1)$$

where E is Young's modulus, E_h is the work-hardening coefficient, and σ_y is the yield stress. In this study, $\sigma_y = E/1000$, $E = 205.9$ GPa, and $E_h/E = 1/100$.

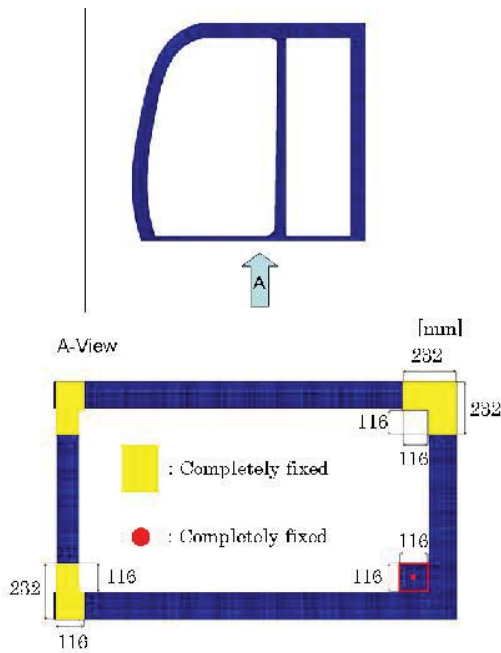


Fig. 2 Constraint condition

B. Analysis Result and Examination

Evaluation method of energy absorption characteristics is by comparing the deformation mode of cab frame and loading part in each analysis conditions. It is conducted with thickness changing of each part. The quantity of energy absorption is observed. The thicknesses of part that is used are 2 mm and 4 mm, with 12 variations using L12 orthogonal array. The combination of each condition is shown in Table I.

TABLE I
THICKNESSES OF PARTS [MM]

Condition	A	B	C	D	E	F	G	H	I	J	K
L12-1	2	2	2	2	2	2	2	2	2	2	2
L12-2	2	2	2	2	2	4	4	4	4	4	4
L12-3	2	2	4	4	4	2	2	2	4	4	4
L12-4	2	4	2	4	4	2	4	4	2	2	4
L12-5	2	4	4	2	4	4	2	4	2	4	2
L12-6	2	4	4	4	2	4	4	2	4	2	2
L12-7	4	2	4	4	2	2	4	4	2	4	2
L12-8	4	2	4	2	4	4	4	2	2	2	4
L12-9	4	2	2	4	4	4	2	4	4	2	2
L12-10	4	4	4	2	2	2	2	4	4	2	4
L12-11	4	4	2	4	2	4	2	2	2	4	4
L12-12	4	4	2	2	4	2	4	2	4	4	2

From FEM analysis results, the thickness conditions are evaluated which generate wrinkling of the cab frame. It is observed that there are 4 locations with wrinkle. Fig. 3 shows the characteristic of deformation at each section. Each deformation mode (each wrinkle occurrence location) is as follows:

- Section (a): wrinkles mode at junction of part A and J.
- Section (b): wrinkles mode at junction of part D and G.
- Section (c): wrinkles mode at both ends of part H.
- Section (d): wrinkles mode at junction of part C and J.

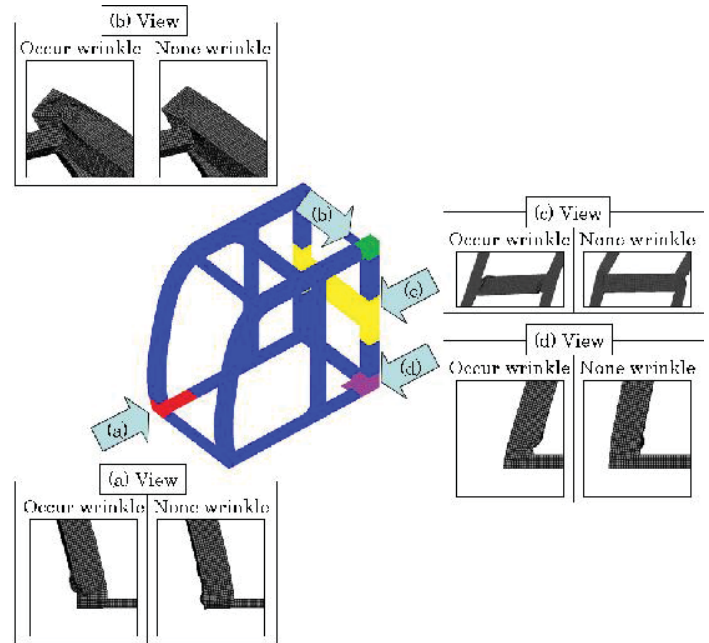


Fig. 3 Deformation View

Figs. 4 and 5 show the comparison of deformation condition on Section (c). Load at deformation mode and displacement diagram are shown in Figs. 6-9. From the displacement-load modes curve, it can be seen that the occurrence of wrinkles could reduce the energy absorption as the following condition:

- Section (a): It has a lower compressive load during 20 ~ 100 mm and more stable load at above 100 mm displacement. The energy absorption is 9.24 MJ reduced (29%).
- Section (b): The wrinkling part only reduce a small amount of compressive load in displacement 100 ~ 500 mm, and energy absorption amount is 4.1 MJ reduced (19%).
- Section (c): The reduction rate of load is higher compared with section (a) and (b). The energy absorption amount when wrinkles part occurred is 9.83 MJ reduced (25%).
- Section (d): The significant reduction of compressive load occurred in this part. Energy absorption amount when wrinkles occur is 21.5 MJ reduced (54%).

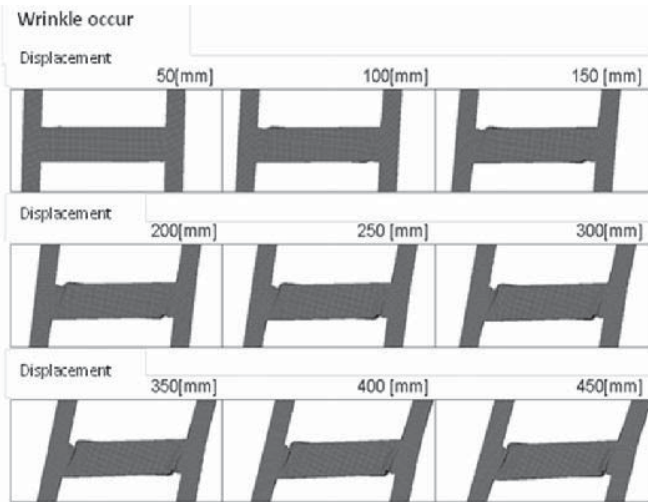


Fig. 4 Deformation condition on part (Section c) - with wrinkle

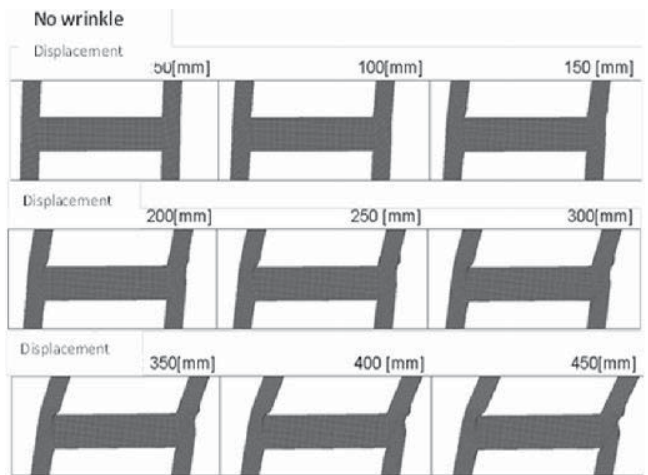


Fig. 5 Deformation condition on part (Section c) - No wrinkle

TABLE II
 DEFORMATION MODE IN EACH CONDITION

Condition	(a)	(b)	(c)	(d)
L12-1	○	○		○
L12-2	○	○		○
L12-3	○		○	
L12-4	○			○
L12-5	○	○		
L12-6	○		○	
L12-7				
L12-8	○	○	○	
L12-9	○			○
L12-10	○	○		
L12-11				○
L12-12		○		○

Wrinkle occurrence of each condition is shown in Table II. The condition with wrinkle occurrence is indicated by ○.

Wrinkle conditions are as follows:

- Section (a): part A or part J is 2 mm,
- Section (b): part D is 2 mm,
- Section (c): part C is 4 mm and part H is 2 mm,

- Section (d): part C is 2mm.

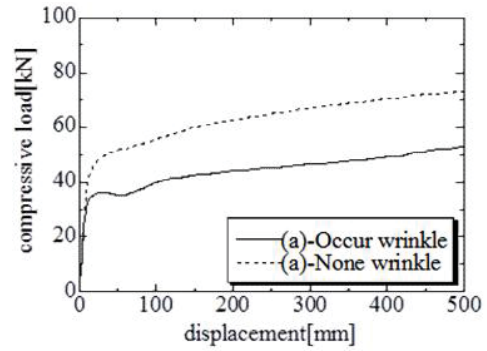


Fig. 6 Load-displacement curve (a)

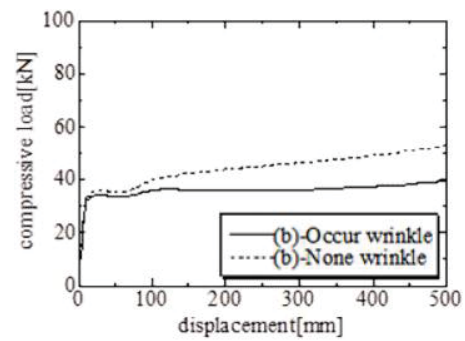


Fig. 7 Load-displacement curve (b)

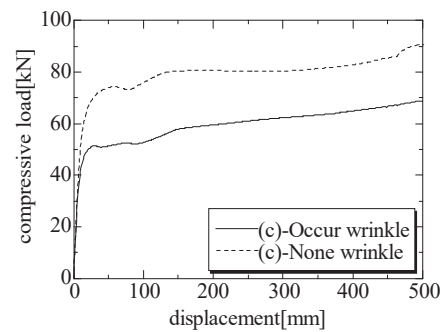


Fig. 8 Load-displacement curve (c)

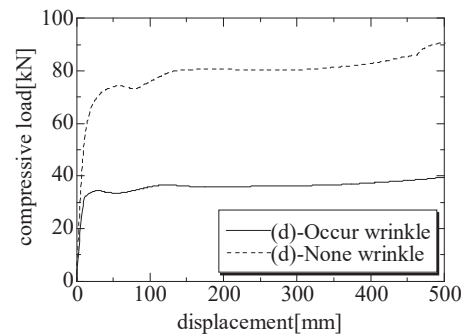


Fig. 9 Load-displacement curve (d)

Figs. 10-13 show the comparison of energy absorption due to difference of deformation mode for sections (a)-(d). Energy

absorptions are reduced when the wrinkle occurs. Energy absorption is significantly reduced at wrinkled section (d). About 60% of energy absorption is decreased.

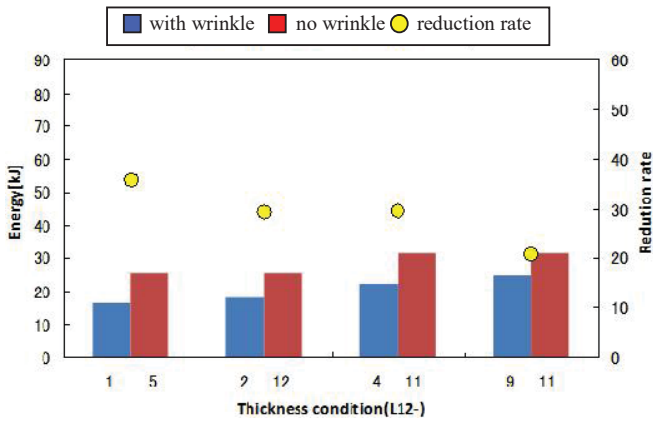


Fig. 10 Comparison of energy absorption due to difference of deformation mode - section (a)

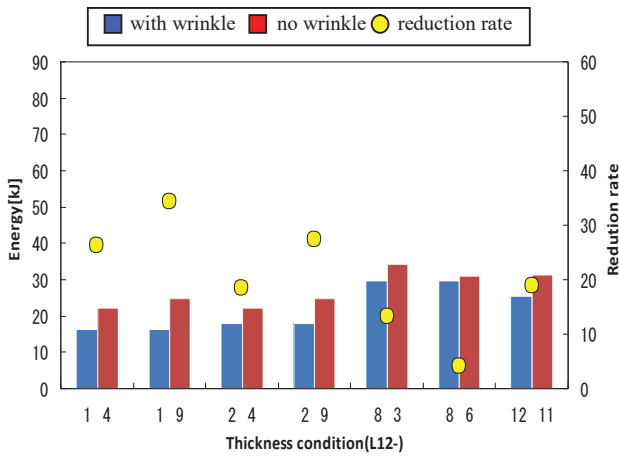


Fig. 11 Comparison of energy absorption due to difference of deformation mode - section (b)

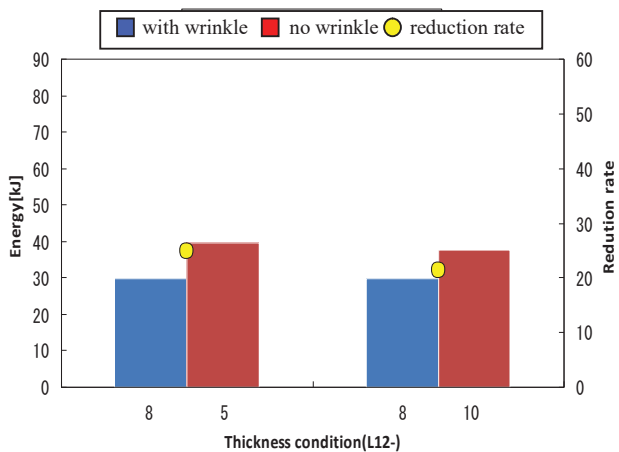


Fig. 12 Comparison of energy absorption due to difference of deformation mode - section (c)

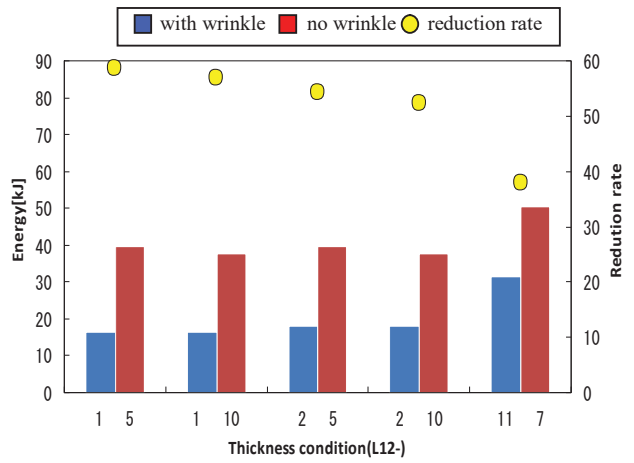


Fig. 13 Comparison of energy absorption due to difference of deformation mode - section (d)

III. MODIFICATION ON PART C

A. Condition Analysis

From analysis results, it is obtained that part C has a significant reduction rate on energy absorption. The modification shape in part C is analyzed. With this modification, new shape can shorten overall length of hydraulic excavator, and it will be easier to pivot in a narrow space. This part is created by bending a straight part (part C), as shown on Fig. 14.

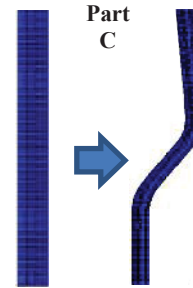


Fig. 14 New shape of cab frame

Boundary conditions and material properties are equal with previous analysis (for straight shape of part C). Using L12 orthogonal array, condition of each part with different thickness is analyzed and the condition with highest energy absorption is used for subsequent analysis. The thickness of part C for all conditions is 6 mm, and the other parts are variations of 2 mm and 4 mm. From FEM analysis results, thickness and wrinkling occurrence of cab frame is evaluated. Different variant is observed at three positions as shown on Fig. 15.

Each of the deformation modes (each wrinkle occurrence location) are as follows.

- Section (a): Part A, wrinkles at junction of J or I.
- Section (b): Part B, wrinkles at junction of D.
- Section (c): Part H, wrinkles at both ends of part H.

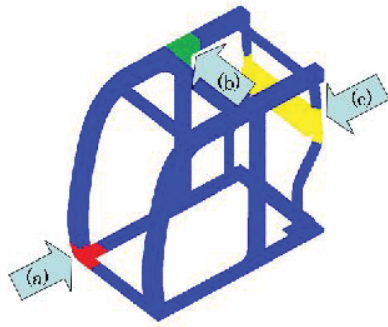


Fig. 15 Location of part observation

The deformation mode for each condition is shown on Table III. The conditions which wrinkle occurred indicated by ○.

TABLE III
 DEFORMATION MODE OCCURRING IN EACH CONDITION

Condition	(a)	(b)	(c)
L12-1	○	○	○
L12-2	○	○	
L12-3	○		○
L12-4	○		
L12-5	○	○	
L12-6	○		○
L12-7			
L12-8	○	○	○
L12-9	○		
L12-10	○	○	
L12-11			○
L12-12		○	○

B.Evaluation of Energy Absorption

Part thickness which wrinkles occurred for each section is section (a): part A or J is 2 mm, Section (b): part D is 2 mm, Section (c): part H is 2 mm.

The characteristic of displacement and load due to wrinkling location is shown in Figs. 16-18. Regardless of occurrence point, load was decreased by occurrence of wrinkles. On sections (a) and (b), we can see similar trend on load. The increment of a load for no wrinkle occurrence at displacement more than 200 mm is slightly different.

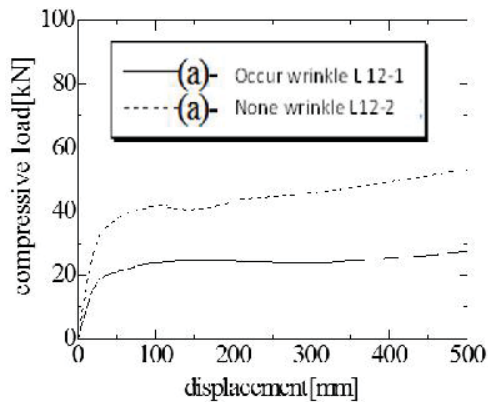


Fig. 16 Effect of wrinkling part (a)

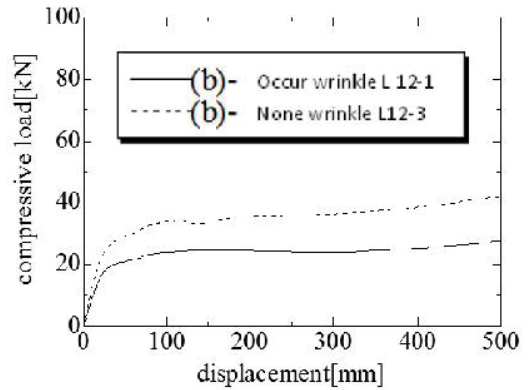


Fig. 17 Effect of wrinkling part (b)

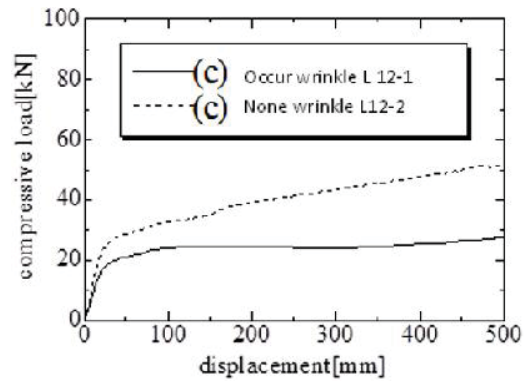


Fig. 18 Effect of wrinkling part (c)

Figs. 19-21 show the comparison of reduction rate and energy absorption amount of each part respectively. If wrinkle occurs, energy absorption was reduced. In section (a), wrinkling make energy absorption amount significantly decreased (about 45%). Conversely, energy absorption decrease by wrinkling section (b) is lower. Thickness conditions that showed the highest energy absorption is L12-7 without occurrence of wrinkles in respective part. Therefore, impact analysis of energy absorbing characteristics due to residual stress using the wall thickness at L12-7.

C.Evaluation of Energy Absorption due to Residual Stress Effect

This section has discussed the effect of energy absorption characteristics of residual stress that generated upon bending. The study of wall thickness is using quadrilateral axis target shell element. Fig. 22 shows residual stress that is generated in part C. Residual stress up to 638 MPa has occurred.

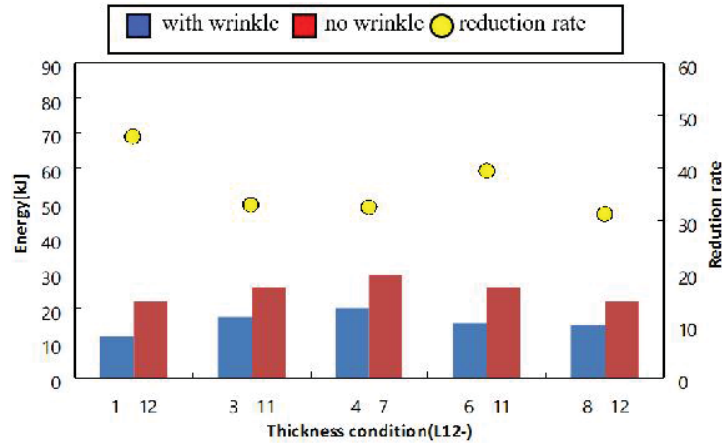


Fig. 19 Comparison of energy absorption due to difference of deformation mode-section (a)

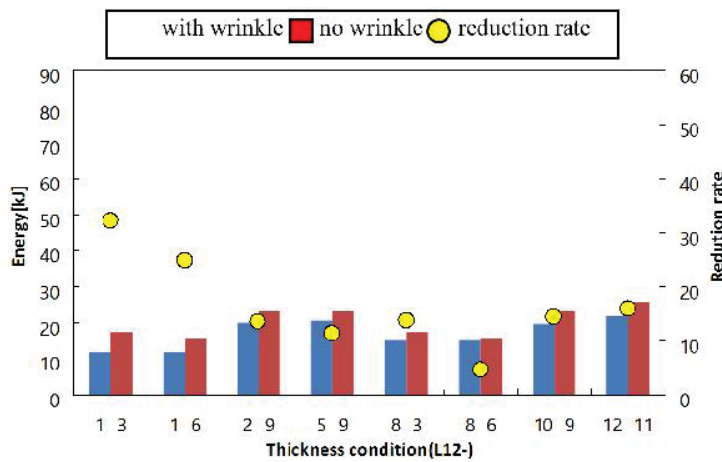


Fig. 20 Comparison of energy absorption due to difference of deformation mode-section (b)

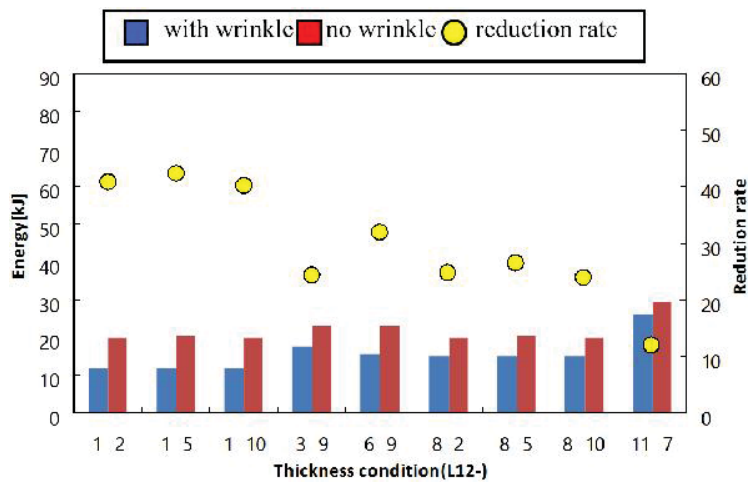


Fig. 21 Comparison of energy absorption due to difference of deformation mode-section (b)

Part C is analyzed by attaching it to cab frame after forming process. Comparison between compressive load and displacement due to residual stress is shown on Fig. 23. Residual stress analysis result shows that residual stress can increase 8% of energy absorption. The energy absorption with residual stress is 2.5 MJ. That is to say the residual stress affects

the energy absorption. It also confirmed that it is possible to increase the energy absorption by forming part.

IV.CONCLUSION

In this study, model with varying thickness of each part of cab frame when fall, use FEM to make elastoplastic numerical

analysis of cab frame. The deformation mode and energy absorption impact of each part were examined. The results are:

- 1) Wrinkles occurred when deforming cab frame can reduce the energy absorption.
- 2) There are 4 wrinkling parts, wrinkles in part C, make the energy absorption significantly reduced.
- 3) It is confirmed that residual stress generated from forming part C is possible to increase the energy absorption.

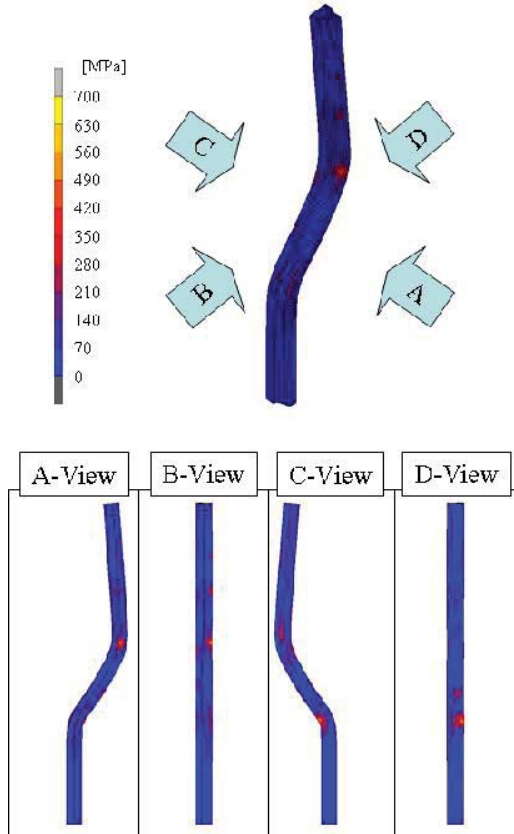


Fig. 22 Residual stress after part C bending process

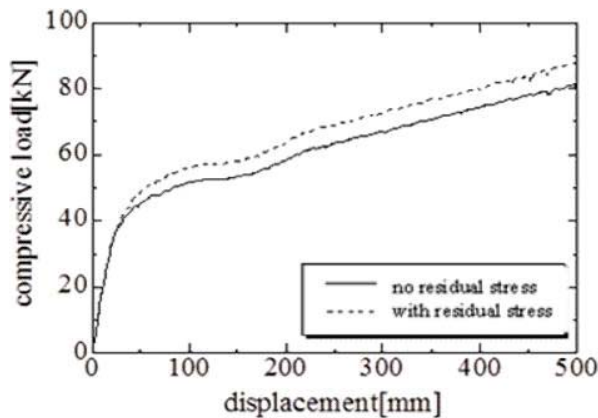


Fig. 23 Load - displacement due to residual stress

ACKNOWLEDGMENT

This project is supported by the Strength of Material laboratory, Yamaguchi University, JSPS KAKENHI Grant

Number 26420079, Japan. The second and third author thank for scholarship support from the Directorate of Higher Education Indonesia cooperated with University of Brawijaya.

REFERENCE

- [1] Sasaki T., "Performance test of operator protective structure (FOPS, ROPS)", construction project, (2011), pp.82-85.
- [2] Kenzo T., "Construction Machinery Fall Protection Structure of Safety Measures Hydraulic Excavator when Rollover (ROPS) up to Japan International Standards", Precision Engineering Journal, Vol.75, No.3 (2009), pp.341-345.
- [3] Hiroshi I., Toshiaki H., "Safety Measures of Construction Machinery", the construction project, (2010), pp.78-81.
- [4] Tadaaki N., Sasaki T., "Research on Large Hydraulic Excavators Fall Protection Structure", construction project, (2004), pp.43-48.
- [5] Kenichi Y., Tsumura D., "Introduction of Hydraulic Excavator Simulation for Driver's Protective Structure Cab during Fallen", Komatsu Technical Report, Vol.52, No.158 (2006), pp.2-7.
- [6] Hiro N.T., Ito T., "ROPS Structure Cab of Production Technology", Komatsu Technical Report, VOL.54, No.161 (2008), pp.9-16.
- [7] Kozeni, T., Haruyama, S., Kaminishi, K., "Study of Energy Absorption of Combined Model of Cylindrical Compression-Expansion Tube and Thin Cylindrical Tube", Proceedings of the 8th International Conference on Innovation & Management, (2011), pp. 1052-1056
- [8] Tawk, I., Rishmany, J., Gergess A., "Assessment of Residual Stresses due to Cold Bending Structural Steel Girders using Finite Element Modeling", Athens Journal of Technology & Engineering, Vol. X, No. Y.
- [9] Prasad, V., Mohan, K., "Finite Element Simulation of Residual Stresses in Roller Bent Section", IJSR, 2013.